Evaluation and Development of the Available Methods of Predicting Capacities of Driven Piles Embedded in Basra Soil

Dr. Haider S. Al-Jubair, Dr. Mushtaq R. Daham

Abstract—The ultimate capacities of single piles utilized in ten projects in Basra-Iraq are evaluated using: various interpretations of pile load test results; several static methods based on site investigation programs; wave equation via (GRLWEAP) and the finite element method via (PLAXIS-3D). For the well-behaved tests, it is realized that the load-settlement data can be best fitted by a hyperbola. Accordingly, Rollberg method well-harmonizes the test results and allows various interpretation methods to be applied on the extrapolated curves. It is found that, the static methods spread over a wide range of values. With a safety factor of (2.8), the allowable capacities of driven piles are estimated properly via the wave equation. Finite element analyses exhibited good agreement to the measured values. It produces failure loads, almost, similar to that obtained from Rollberg method. The finite element analyses revealed local settlement of (2% - 3.3%) of the pile section width to mobilize the ultimate skin resistance. The necessary pile-head settlement for producing the ultimate frictional point resistance is (13% - 22.4%) of the pile section width. Graphical relationships are suggested to obtain the adhesion and friction factors, deduced from the finite element method. Utilizing those relations to predict the skin resistance component with Meyerhof's (1976) method to calculate the bearing component, gives suitable allowable capacities by applying a safety factor of (5). The maximum related settlement is (5.5 mm) which is equivalent to (0.6%) of the pile section width and is tolerable for most types of structures.

Index Terms— Driven piles, Ultimate capacity, Static approach, Wave equation, skin resistance, point bearing, Finite element

———————————— u ————————————

2 INTRODUCTIONS

PILE foundations are widely used in Basra city due to the presence of a shallow saturated soft cohesive soil layer of variable thickness in soil profile.

In order to provide the geotechnical engineers with reliable estimates to the ultimate compressive capacity of vertical piles driven in Basra soil, the following tasks are accomplished:

1. The available equations derived based on the static approach are evaluated to select / modify the most adequate ones.
2. The dynamic wave equation method is evaluated.
3. The methods of interpreting the static pile load test data are assessed to indicate the most favorable ones.
4. The soil-pile interaction behavior is investigated via the finite element models.

The area covered by the study is located within the administrative, commercial, and residential center of Basra city. Ten projects utilizing driven pile foundations are considered as case studies for the verified methods Figure (1). The provided data sets from those projects include: geotechnical investigation reports; driving records; and load test data, for trial and/or working piles.

Fig. 1. Locations of the projects taken into consideration

2 STATIC APPROACH

For a pile of (n) segments and/or penetrating a soil profile of (n) sublayers, the ultimate compressive capacity can be expressed as [4] and [5]:

$$Q_u = Q_p + Q_s = q_p * A_p + \sum_{i=1}^{n} q_{si} * A_{si}$$

Where:

Q_u: ultimate load capacity
Q_p: ultimate point capacity
Q_s: ultimate skin resistance
q_p: unit point resistance
A_p: area of the pile point
q_{si}: unit shaft resistance within the segment or sublayer (i)
A_{si}: corresponding surface area

The point resistance per unit area is usually calculated as:

International Journal of Scientific & Engineering Research Volume 10, Issue 1, January-2019
ISSN 2229-5518

$$q_p = c\ N_c' + \sigma_o' N_q'$$

Where:

N_c' , N_q': bearing capacity factors adjusted for depth and shape.

σ_o': effective overburden pressure at pile point.

c : soil cohesion around pile point.

φ: soil angle of internal friction.

The (N'c) factor could be predicted using the formula [12]:

$$N'_c = 6 + \frac{L}{D} \leq 9$$

Whereas the (*N'q*) factor can be obtained from Figure (2). The unit point resistance can also be predicted based on the standard penetration number as [2]:

$$q_p = 40\ N_{55} \frac{L}{D} \leq 400\ N_{55}$$

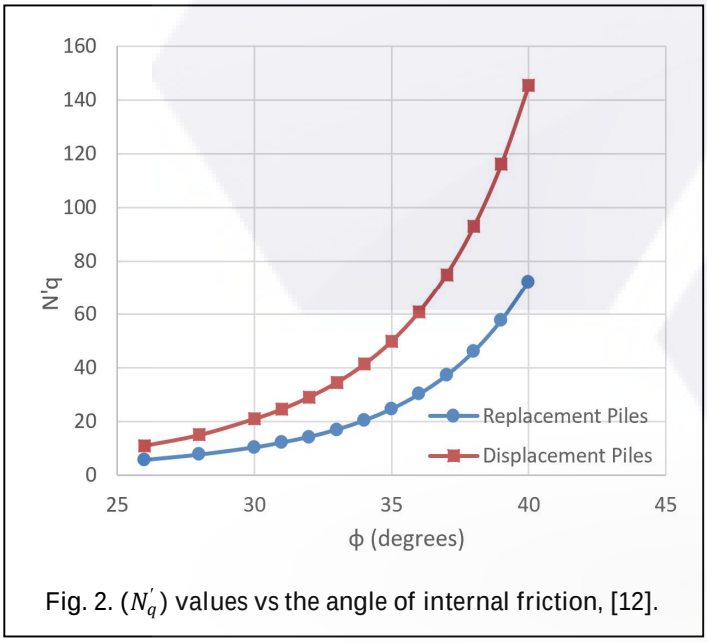

Fig. 2. (N_q') values vs the angle of internal friction, [12].

$$q_s = \alpha\, c + K\sigma_{oav}' \tan\delta = \alpha\, c_u + \beta\sigma_{oav}'$$

Where:

α: adhesion factor.

σ_{oav}': effective overburden pressure at the mid-depth of penetration in soil layer.

K: lateral earth pressure coefficient.

δ: friction angle between the soil and pile material.

φ: soil angle of internal friction.

The values or formulas for estimating the necessary parameters, suggested by different authors are summarized in Table (1). The unit skin resistance can also be predicted based on the standard penetration number as [5]:

$$q_s = 2N_{60}$$

or [3]:

$$q_s = (4\ to\ 5)N_{60}$$

TABLE 1

SUMMARY OF THE SKIN RESISTANCE PARAMETERS

Cohesive Component			
Source	α		Range of application
Tomlinson (1956) [8]	$0.20 + 0.20(\frac{P_A}{c_u})$		$25\ kPa < c_u < 200\ kPa$
	1		$c_u \leq 25kPa$
	0.3		$c_u \geq 200kPa$
Randolph and Murphy (1985), as cited by [13]	$\left(\frac{c_u}{\sigma'_{oav}}\right)_{NC}^{0.5}\left(\frac{c_u}{\sigma'_{oav}}\right)^{-0.5}$		$\frac{c_u}{\sigma'_{oav}} \leq 1$
	$\left(\frac{c_u}{\sigma'_{oav}}\right)_{NC}^{0.5}\left(\frac{c_u}{\sigma'_{oav}}\right)^{-0.25}$		$\frac{c_u}{\sigma'_{oav}} \geq 1$
Viggiani (1993) [13]	$1 - \frac{c_u - 25}{90}$		$25kPa < c_u < 70kPa$
	1.0		$c_u \leq 25kPa$
	0.5		$c_u \geq 70kPa$
P_A: atmospheric pressure (P_A=100 kPa).			
NC: normally consolidated			
Friction Component			
Source	K		δ
Go &Oleson (1993) [13]	$K = 0.9 + 0.02N_{60}$		
Tomlinson and Woodward (2015) [12]	K $= (1to2)\ (1 - \sin\varphi)$		
Broms Method [13]	Steel	0.5-1.0	Steel 20°
	Concrete	1.0-2.0	Concrete 0.75φ

3 WAVE EQUATION

The wave equation analysis is based on the theory of propagation of the linear waves (Figure 3). In this approach, the pile behavior during driving is modelled, considering

International Journal of Scientific & Engineering Research Volume 10, Issue 1, January-2019
ISSN 2229-5518

factors such as driving energy delivered to the pile at impact, propagation of compressive and tensile waves, soil static resistance along the pile shaft and resistance below the pile toe, as well as dynamic behavior of soil as a viscous body. The basic wave equations for pile driving analysis are [14]:

$$D(m,t) = D(m,t-1) + \Delta t\, v(m,t-1)$$
$$C(m,t) = D(m,t) - D(m+1,t)$$
$$F(m,t) = C(m,t) + K(m)$$

$$v(m,t) = v(m,t-1) + [F(m-1,t) + W(m) - F(m,t) - R(m,t)]\frac{g\Delta t}{W(m)}$$

With no damping:

$$R(m,t) = [D(m,t) - D'(m,t)]K'(m)[1 + J(m)\, v(m,t-1)]$$

With damping:

$$D(m,t) = G'(m)$$
$$R(m,t) = [D(m,t) - D'(m,t)]K'(m) + J(m)R_{su}(m)\, v(m,t-1)]$$

Where:

m: element number
t: time
g: acceleration caused by gravity
$K(m)$: spring constant for internal spring m
$W(m)$: weight of the element m
$v(m,t)$: velocity of element m at time t
$D(m,t)$: displacement of element m at time t
$D'(m,t)$: plastic displacement of external spring (i.e. the surrounding ground) m at time t
$R(m,t)$: force exerted by external spring m on element m at time t
$R_d(m)$: dynamic resistance of element m
$J(m)$: soil-damping constant at element m
Δt: time interval considered
$C(m,t)$: compression of internal spring m at time t

$K'(m)$: spring constant for external spring m
$F(m,t)$: force in internal spring at time t
$v(m,t-1)$: velocity of element at time t-1
$D(m,t-1)$: displacement of element m at time t-1
$G'(m)$: quake for external spring m (or maximum elastic soil deformation)
$R_{su}(m)$: ultimate static resistance of external soil spring m

A licensed package of the latest version of GRLWEAP from PDI [6] is utilized for the present research.

4 Pile Load Tests

The most common test procedure in Iraq is the slow maintained load test according to the ASTM-D1143 [1]. The true failure occurs when the pile plunges down into the ground without any further increase in load [12] but, many settlement-based failure criteria have been defined. Other interpretation methods have been developed like [9], [11]: Davisson; Chin; Hansen (80% and 90%); Dee-Beer; Fuller and Hoy; Butler and Hoy; Van der Veen; and Rollberg methods.

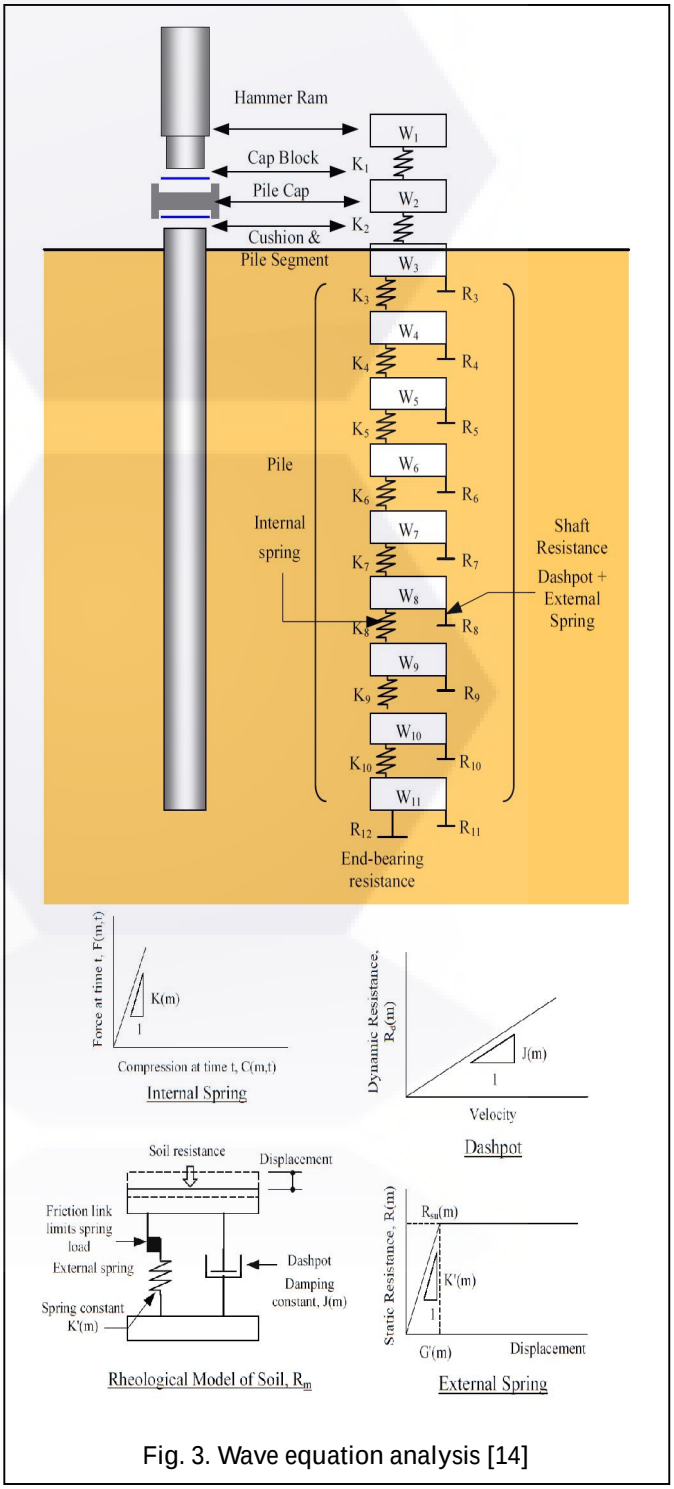

Fig. 3. Wave equation analysis [14]

International Journal of Scientific & Engineering Research Volume 10, Issue 1, January-2019
ISSN 2229-5518

5 Finite Element Method

For the three-dimensional stress analysis, the matrix equations are [10]:

$$[\underline{K}]\underline{\vec{Q}} = \underline{\vec{P}}$$

Where:

$[\underline{K}]$ =global stiffness matrix
$\underline{\vec{Q}}$ =global vector of nodal displacements
$\underline{\vec{P}}$ = global nodal load vector

$$[\underline{K}] = \sum_{e=1}^{n}[K^{(e)}]$$

$$\underline{\vec{P}} = \underline{\vec{P}_c} + \sum_{e=1}^{n}\vec{P}_i^{(e)} + \sum_{e=1}^{n}\vec{P}_s^{(e)} + \sum_{e=1}^{n}\vec{P}_b^{(e)}$$

$$[K^{(e)}] = \iiint_{V^{(e)}}[B]^T[D^{ep}][B]\,dV$$

$\vec{P}_i^{(e)} = \iiint_{V^{(e)}}[B]^T[D]\vec{\epsilon}_\circ\,dV$ = element load vector due to initial strain

$\vec{P}_s^{(e)} = \iint_{S_1^{(e)}}[N]^T\overrightarrow{\overrightarrow{\Phi}}\,dS_1$ = element load vector due to surface forces

$\vec{P}_b^{(e)} = \iiint_{V^{(e)}}[N]^T\overrightarrow{\overrightarrow{\emptyset}}\,dV$ = element load vector due to body forces

$[K^{(e)}]$ = element stiffness matrix
$\underline{\vec{P}_c}$ = vector of concentrated loads
V = the volume of the body
n = number of elements
$[N]$ = shape function
$\overrightarrow{\varepsilon_0}$ = vector of initial strains
S_1 = the surface of the body

A time limited license of PLAXIS-3D Foundation (2015) is used in the current study. The soil is modeled using Mohr-Coulomb criterion whereas, a linear elastic model is selected to represent pile material. In order to reduce the effect of boundaries on the results, the soil media are extended to minimum distances of ten times pile width from the pile edge in the lateral directions, and five times pile width below the pile tip [4]. Soil properties are drawn from the geotechnical investigation reports and some parameters are specified based on correlative relations in case of lack of data [15-34].

6 Discussion to The Results

All the input data and output results are presented for the first project only. For the remaining nine projects, partial inputs / outputs are presented in the summary Tables. The first project is a multistory surgical complex building supported on (400mm x 400mm x 24m) precast concrete piles, driven via a diesel hammer (Delmag D22) into the soil profile shown in Figure (4) [15]. The measured load-settlement curve is shown in Figure (5) [16]. The ultimate load capacities obtained from the various interpretation methods are shown in Figures (6) through (11).

It is realized that a test load of (2700 kN), which is equivalent to (300%) the design load, could not bring the pile to plunging. The ultimate loads obtained by Davisson's method (2330.0 kN) and according to a net settlement of (0.25 in = 6.35 mm) (2560.0 kN), are within the range of test load. Other methods revealed values exceeded that load, such as Chin's (3225.0 kN), Brinch Hansen's 80% (2887.0 kN), and Van der Veen's (2750.0 kN) methods.

Rollberg method has the ability to extrapolate the load-settlement curve beyond the maximum test load to the plunging limit. This provides the possibility to examine many settlement-based failure criteria. Accordingly, the ultimate capacities based on pre-assigned pile-butt settlement values equivalent to [(6% B), (Elastic + B/30), (10% B) and (20% B)] are [(2595.0 kN), (2693.0 kN), (2807.0 kN) and (3230.0 kN)], respectively.

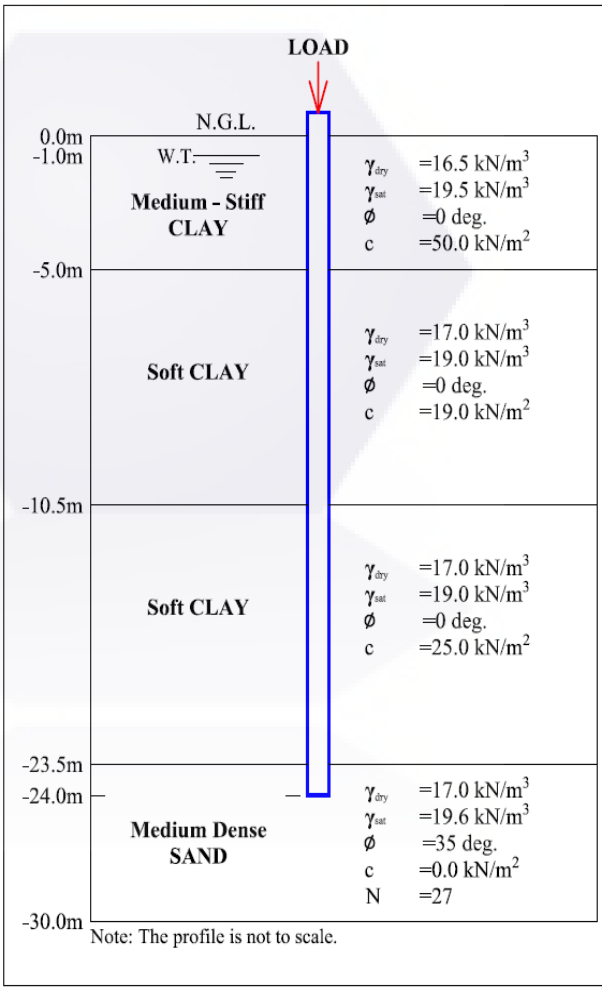

Fig. 4. Soil-pile profile (project No. 1)

International Journal of Scientific & Engineering Research Volume 10, Issue 1, January-2019
ISSN 2229-5518

-settlement curve is shown in Figure (5) [16]. The ultimate load capacities obtained from the various interpretation methods are shown in Figures (6) through (11).

It is realized that a test load of (2700 kN), which is equivalent to (300%) the design load, could not bring the pile to plunging. The ultimate loads obtained by Davisson's method (2330.0 kN) and according to a net settlement of (0.25 in = 6.35 mm) (2560.0 kN), are within the range of test load. Other methods revealed values exceeded that load, such as Chin's (3225.0 kN), Brinch Hansen's 80% (2887.0 kN), and Van der Veen's (2750.0 kN) methods.

Rollberg method has the ability to extrapolate the load-settlement curve beyond the maximum test load to the plunging limit. This provides the possibility to examine many settlement-based failure criteria. Accordingly, the ultimate capacities based on pre-assigned pile-butt settlement values equivalent to [(6% B), (Elastic + B/30), (10% B) and (20% B)] are [(2595.0 kN), (2693.0 kN), (2807.0 kN) and (3230.0 kN)], respectively.

It is clear that, the Chin's capacity is very close to the plunging load, as calculated via Rollberg extrapolated curve at a settlement of (80 mm = 20% B). The ultimate Vander Veen's and Brinch Hansen's 80% capacities are very close to the Rollberg's value associated with a settlement of (40 mm = 10% B).

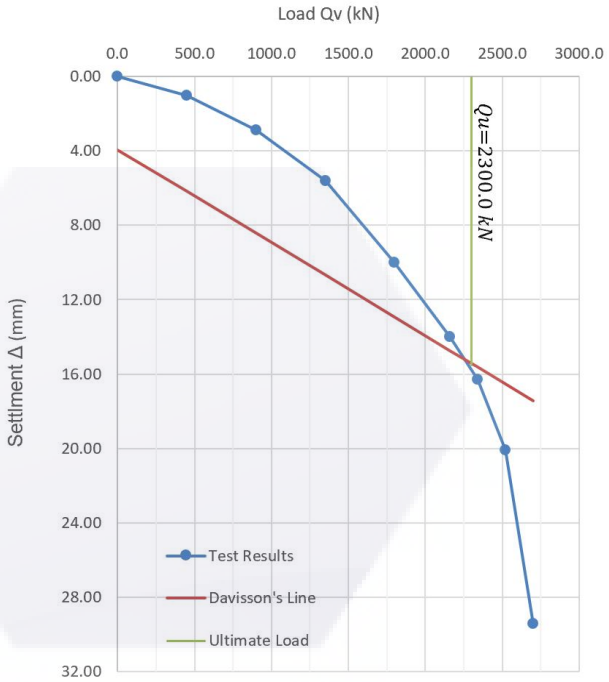

Fig. 6. Ultimate pile capacity by Davisson's method (project No. 1)

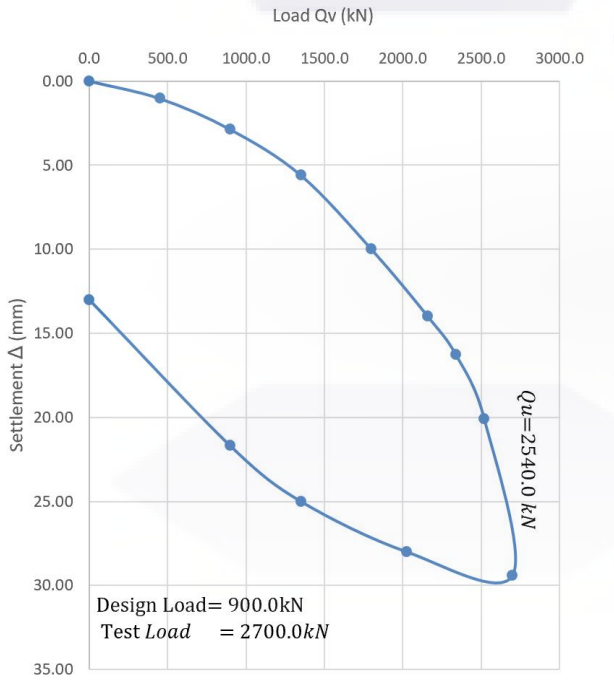

Fig. 5. Ultimate pile capacity by Davisson's method (project No. 1)

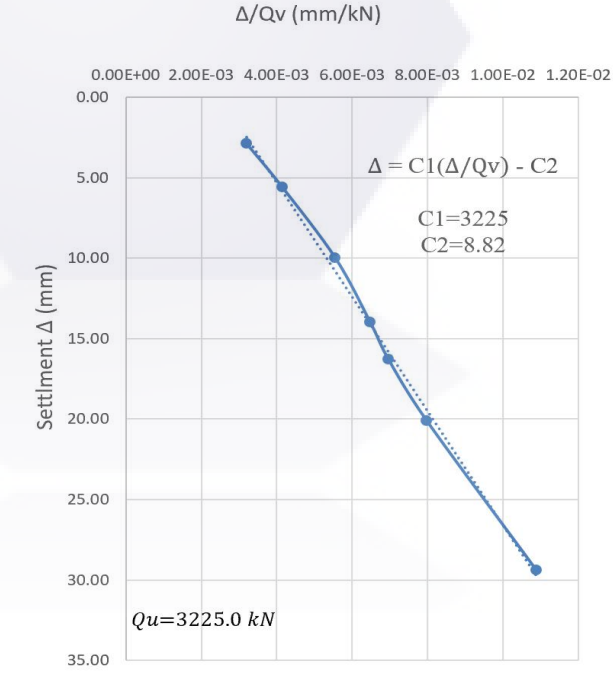

Fig. 7. Ultimate pile capacity by Chin's method (project No. 1).

International Journal of Scientific & Engineering Research Volume 10, Issue 1, January-2019
ISSN 2229-5518

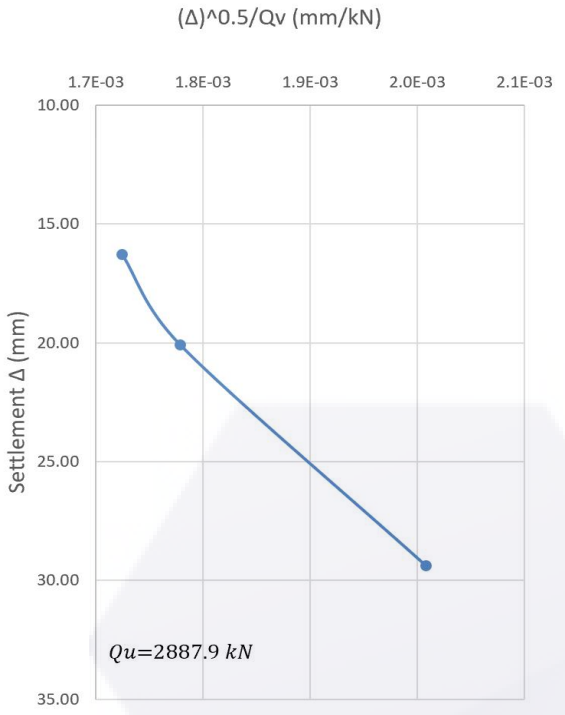

Fig. 8. Ultimate pile capacity by Brinch Hansen's 80% method (project No. 1).

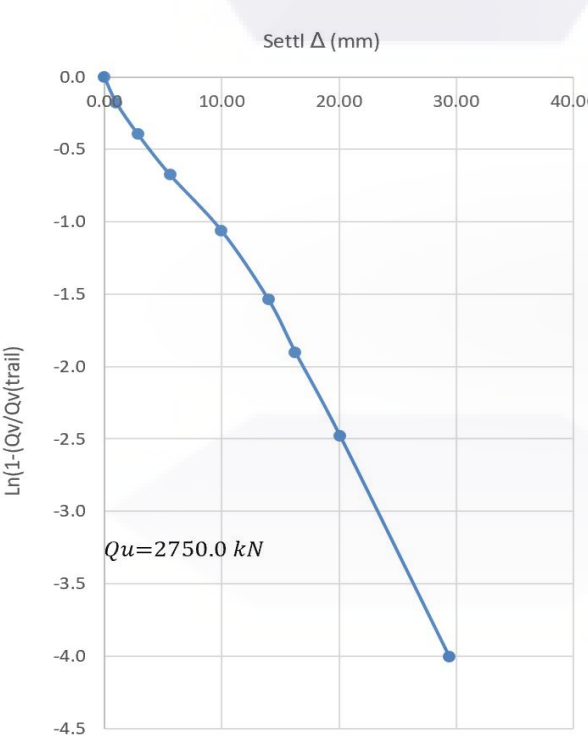

Fig. 9. Ultimate pile capacity by Vander-Veen's method (project No. 1)

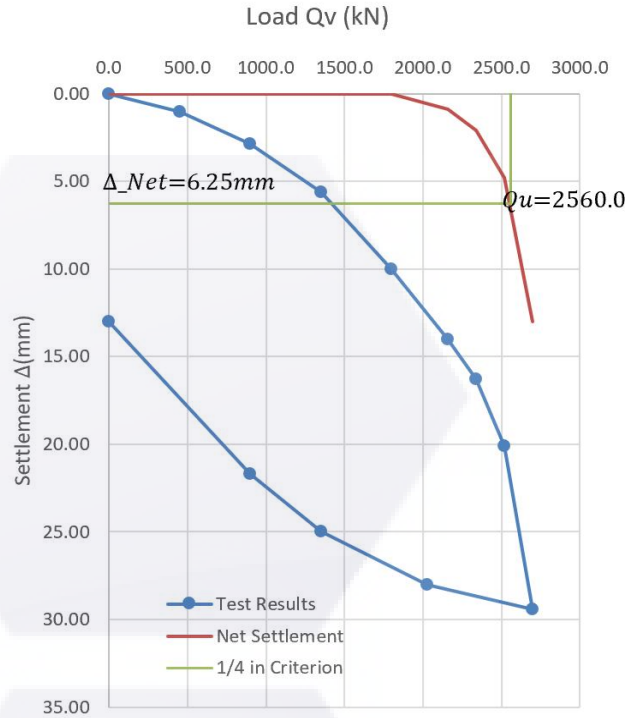

Fig. 10. Ultimate pile capacity based on net-settlement criterion (project No. 1).

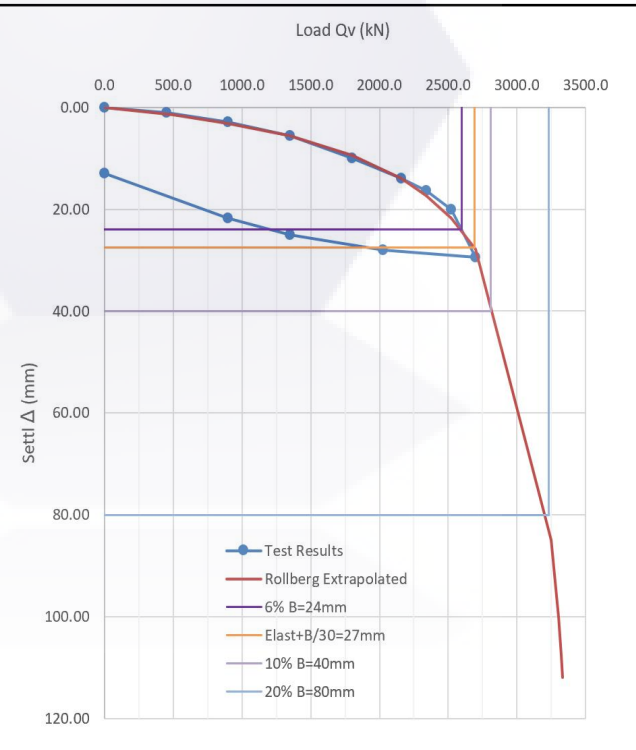

Fig. 11. Ultimate pile capacity by Rollberg's method (project No. 1).

International Journal of Scientific & Engineering Research Volume 10, Issue 1, January-2019
ISSN 2229-5518

The ultimate capacities, produced by Davisson's method and the net settlement criterion, are the most conservative among the values obtained from the applicable methods. The range of test load and the produced slopes rendered Brinch Hansen's 90%, De Beer's, Fuller & Hoy's and Butler & Hoy's methods inapplicable for this project.

The existence of numerous static methods for skin and point resistances estimation produce a big number of combinations for pile capacities. The maximum and minimum capacities are summarized in Table (2).

TABLE 2

Ultimate extremum values by the static methods (project No. 1).

Method / Resistance Component	Minimum values		Maximum values	
	Method	Value (kN)	Method	Value (kN)
Skin Resistance (Cohesive)	Tomlinson [8]	927.2	Randolph [13]	1087.2
Skin Resistance (Cohesionless)	Meyerhof [5].	43.2	Nordlund [9]	156.2
Point Bearing	Meyerhof [2]	216.0	Meyerhof [12]	1836.3
Total Ultimate Capacity	1186.4		3079.7	

The minimum ultimate static load underestimates the true capacity whereas, the maximum value is very close to its load-test counterpart, obtained from the (16% B) settlement criterion. The skin resistance component ranges from (970.4 kN) to (1243.4 kN) while, the point bearing component ranges from (216.0 kN) to (1836.3 kN). These two components shall be further discussed after the presentation of the finite element results.

The results of the wave equation shown in Figure (12) gives an ultimate capacity of (3100.0 kN), which is close to the plunging load, with a skin resistance of about (43% Qu =1333 kN) and a point bearing of (57% Qu =1767 kN). It is also shown that, the pile driving induced compressive stresses in the pile material reached (36.75 MPa), which exceeds the recommended allowable value [2] of (0.85 f_c' = 34.0 MPa). This gives an indication of overdriving (very low set value).

The input parameters for the finite element analysis are listed in Table (3). The finite element mesh is shown in Figure (13) whereas, the displacement contours are demonstrated in Figure (14) for a sample load. The predicted behavior is compared to the measured one in Figure (15) whereas, the computed load-settlement curves for the different resistance components are shown in Figure (16). The analysis is terminated at an ultimate load of (3157.9 kN).

Figure (17) illustrate the load transferred from pile to soil, whereas the variations of pile displacement with depth are illustrated in Figure (18), for various multiples of the design load. It is realized that at the design load, the point bearing has no contribution in load resistance which is restricted to the skin component, which is fully mobilized at a butt settlement of around (11mm = 2.8% B) or local displacement around (9mm = 2.3% B), and an applied load of (250% Q_{design}). The point bearing component continues to increase and reaching its maximum value at a butt settlement of around (89 mm = 22.2% B), which is associated with plunging.

The contributions of soil layers in skin resistance are calculated from the load differences at layer boundaries. The results are listed in Table (4). According to the transferred force within each layer and the associated pile surface area, the skin resistance parameters (α_i and β) are back calculated for the static method, from the finite element results, as:

$$a_i = \frac{Qs_i}{As_i' \, c_{ui}}$$

$$b = K \cdot \tan d = \frac{Qs_4}{As_4' \, s'_{av4}}$$

and the results are listed in Table (5). Adhesion factors of (1.04) for medium stiff clay is uncommon value, whereas, values of (1.23) and (1.14) for soft clayey layers of cohesion (19kN/m²) and (25kN/m²), respectively are frequent. In addition to that, the predicted β-value gives high unit shear stress within the cohesionless layer that exceeds the limit of (100 kPa), which is recommended by many references.

Conclusions

For the studied ten projects, the following conclusions can be drawn:

1. Pile load tests in Basrah are usually used as proof tests, even for the trial piles. Piles are rarely tested to failure.
2. For a well-conducted tests (with no problems), the load-settlement data can be fitted with a considerable degree of accuracy by a hyperbola. According to that, Rollberg method simulates the test results in a good manner and permits the application of many interpretation criteria on the extrapolated curves.

International Journal of Scientific & Engineering Research Volume 10, Issue 1, January-2019
ISSN 2229-5518

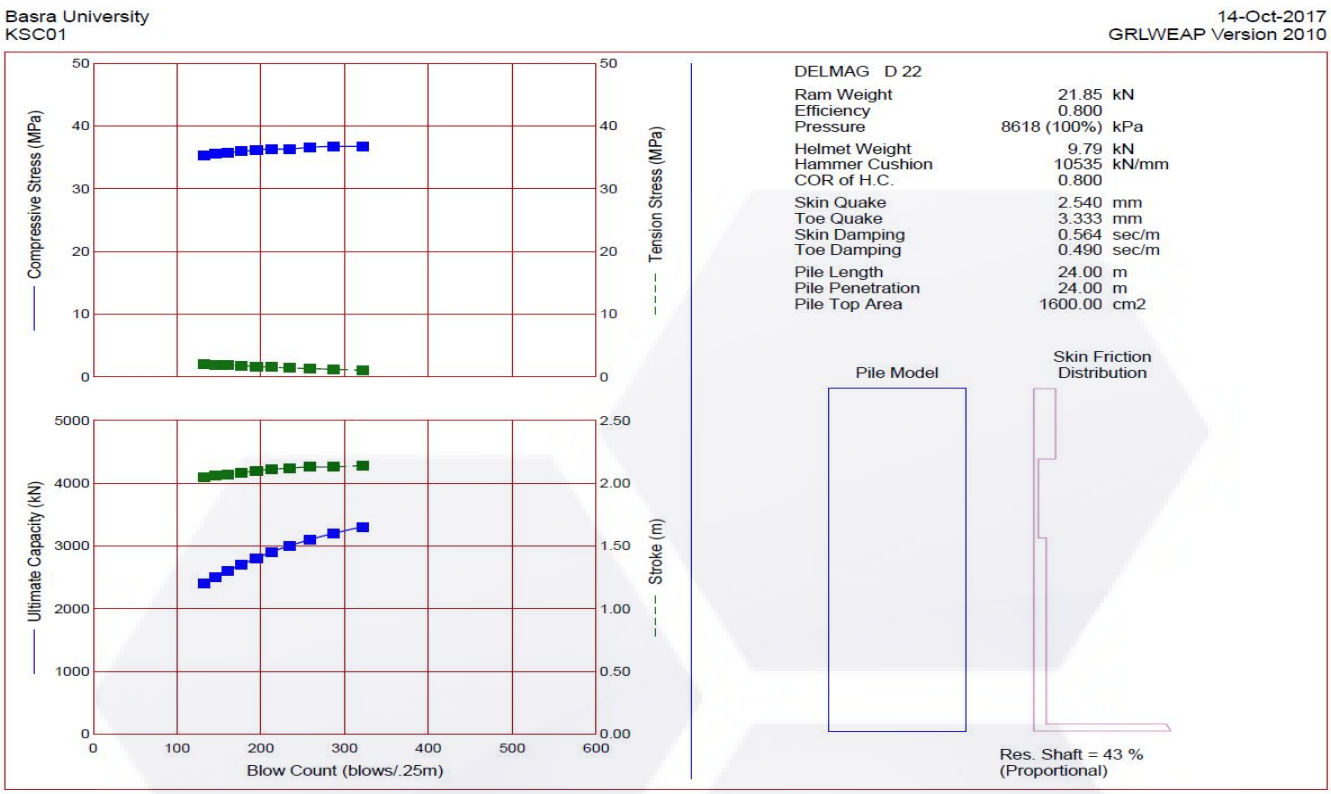

Basra University
KSC01

14-Oct-2017
GRLWEAP Version 2010

Ultimate Capacity kN	Maximum Compression Stress MPa	Maximum Tension Stress MPa	Blow Count blows/.25m	Stroke m	Energy kN-m
2400.0	35.35	1.96	132.8	2.05	20.79
2500.0	35.59	1.92	145.7	2.06	20.78
2600.0	35.71	1.86	160.2	2.07	20.85
2700.0	35.98	1.76	176.9	2.08	20.88
2800.0	36.11	1.65	194.6	2.10	20.94
2900.0	36.36	1.53	212.9	2.11	20.99
3000.0	36.34	1.41	234.2	2.12	21.00
3100.0	36.60	1.30	258.3	2.13	21.05
3200.0	36.75	1.18	287.1	2.13	21.07
3300.0	36.76	1.06	321.3	2.14	21.08

Fig. 12. Ultimate pile capacity by the wave equation (project No. 1)

International Journal of Scientific & Engineering Research Volume 10, Issue 1, January-2019
ISSN 2229-5518

TABLE 3

Input parameters of Finite element analysis (project No. 1).

Parameter	Symbol	Unit	Medium Stiff Clay (0.0-5.0) m	Soft Clay (5.0-10.5) m	Soft Clay (10.5-23.5)m	Medium Dense Sand (23.5-30.0)m	Driven Pile (400x400)mm² (0.0-24.0)m
Material F.E. Model	Model	--	Mohr-Coulomb	Mohr-Coulomb	Mohr-Coulomb	Mohr-Coulomb	Liner Elastic
Drainage Type	Type	--	Undrained	Undrained	Undrained	Drained	Non-porous
Unit weight above phreatic level	γ_{unsat}	kN/m³	16.5	17.0	17.0	17.0	24.0
Unit weight under phreatic level	γ_{sat}	kN/m³	19.5	19.0	19.0	19.6	24.0
Young's Modulus	E'	MN/m²	30.0	8.5	15.0	37.0	30 000
Poisson's Ratio	ν'	--	0.30	0.37	0.35	0.27	0.15
Cohesion	c_u	kN/m²	50.0	19.0	25.0	0.0	N/A
Friction Angle	φ'	Degree	0.0	0.0	0.0	35.0	N/A
Dilatancy Angle	ψ'	Degree	0.0	0.0	0.0	5.0	N/A
Lateral Earth Pressure Coefficient	k_0	--	1.0	1.0	1.0	0.426	N/A

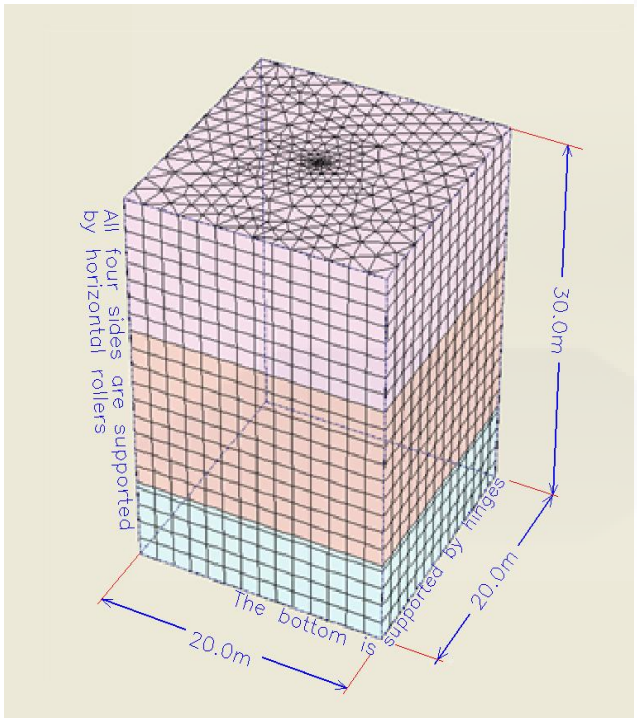

Fig. 13. Finite element mesh (project 1)

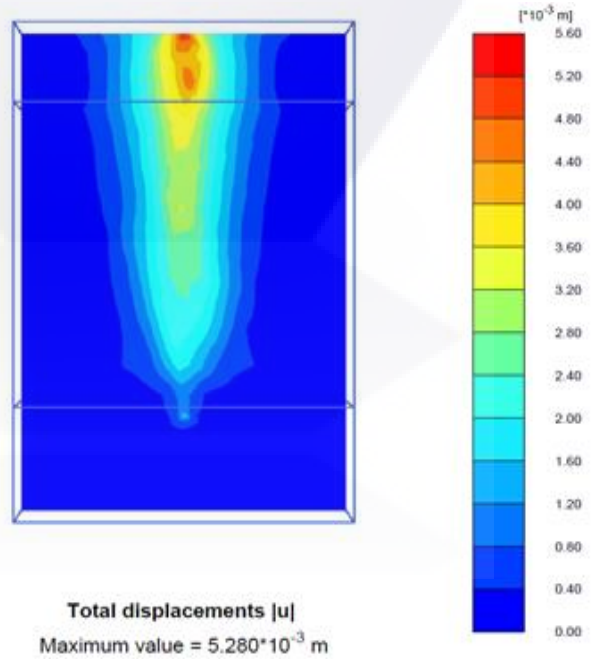

Fig. 14. Displacement contours at an applied load of (1700.0 kN) (project No. 1). [12].

International Journal of Scientific & Engineering Research Volume 10, Issue 1, January-2019
ISSN 2229-5518

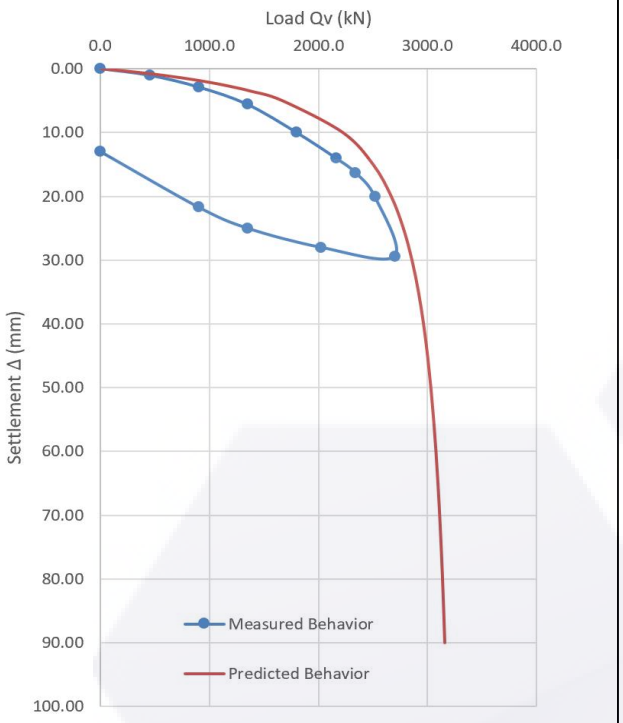

Fig. 15. Predicted load-settlement curve vs measured one (project No. 1).

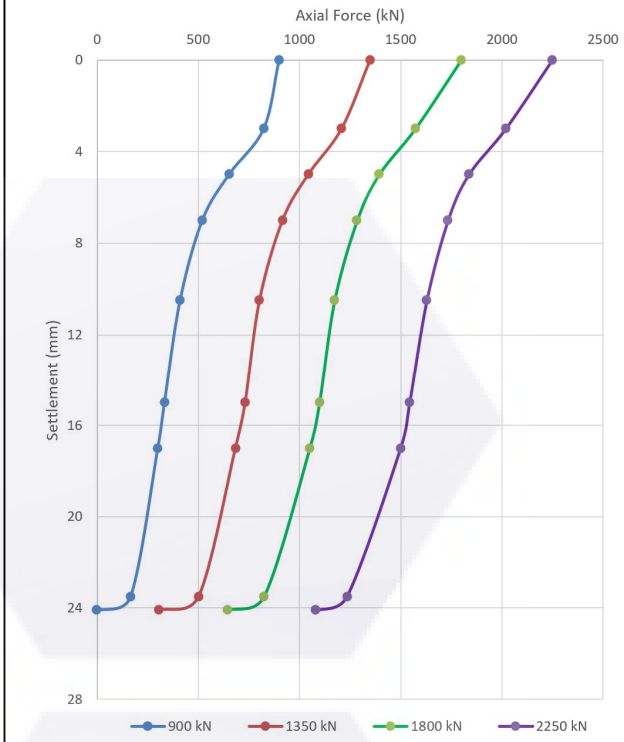

Fig. 17. Load transfer vs depth (project No. 1)

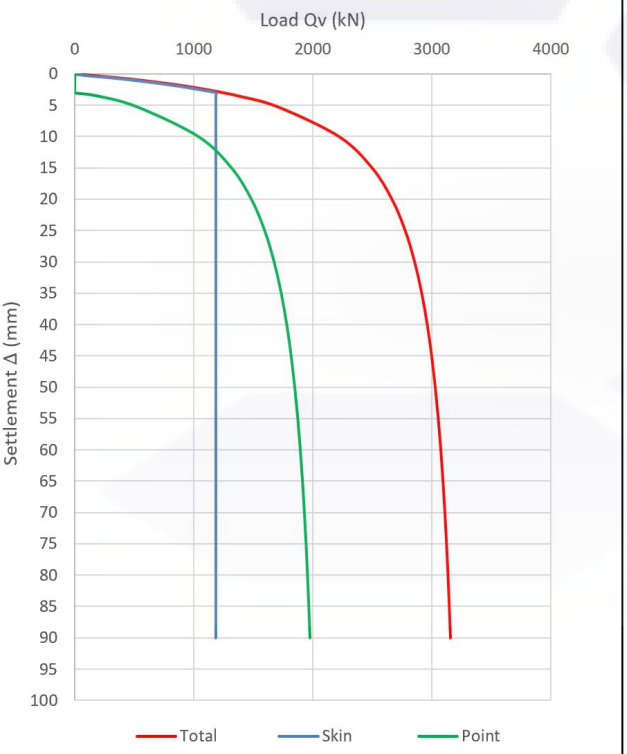

Fig. 16. Predicted ultimate capacities (project No. 1).

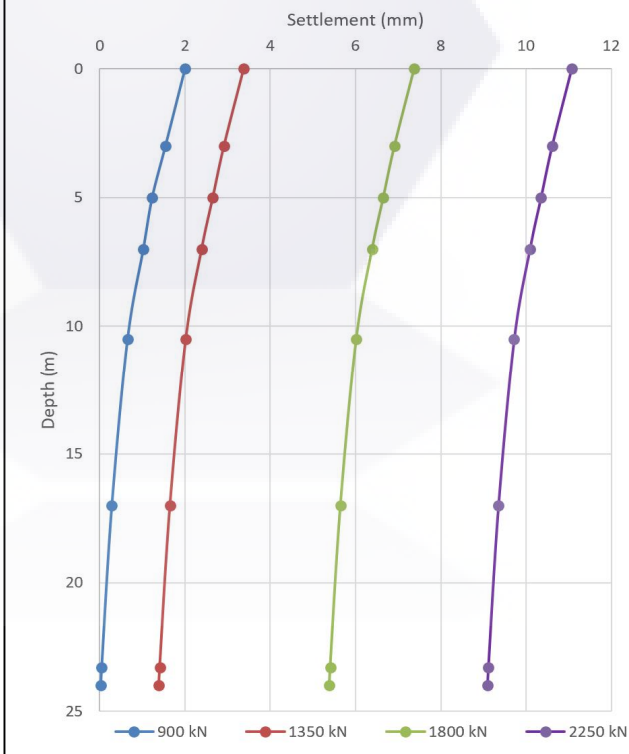

Fig. 18. Pile displacement versus depth (project No. 1)

International Journal of Scientific & Engineering Research Volume 10, Issue 1, January-2019
ISSN 2229-5518

TABLE 4

Contributions of soil layers in load resistance (project No. 1)

Depth (m)	0 to 5	5 to 10.5	10.5 to 23.5	23.5 to 24.1	Skin Resistance		Point Bearing	
Load (kN)	Qs_1	Qs_2	Qs_3	Qs_4	Value	%	Value	%
900	248	242	245	165	900	100.0	0	0.0
1350	306	241	301	197	1045	77.4	305	22.6
1800	406	221	349	179	1155	64.2	645	35.8
2250	412	208	395	155	1170	52.0	1080	48.0
2700	415	205	580	150	1350	50.0	1350	50.0
3000	415	205	593	155	1368	45.6	1632	54.4
3157.9					1183.7	37.5	1974.2	62.5

TABLE 5

Predicted skin resistance parameters (project No. 1).

Load (kN)	α_1 for c_{u1}=50 kPa	α_2 for c_{u2}=19 kPa	α_3 for c_{u3}=25 kPa	β for N=27
2250	1.03	1.24	0.76	0.82
2700	1.04	1.23	1.12	0.82
3000	1.04	1.23	1.14	0.84
3157.9	1.04	1.23	1.14	0.84

TABLE 6

Summary of the interpretations, static, and dynamic methods

Project No.	1	2	3	4*	5	6	7	8	9	10
Pile dimensions mm^2 x m	400^2x24	285^2x20	400^2x23	285^2x26	285^2x26	285^2x24	285^2x21	285^2x21	285^2x21	285^2x22
Load Test										
D/T load (kN)	900/2700	400/800	750/1500	350/525	400/1200	400/1200	350/700	300/900	350/700	350/700
Davisson	2330								675	
Chin	3225	1243	2522	1266	1713	1812	1537	1696	901	1268
Hansen 80%	2887	995	1886	986	1418				750	805
Vander-Veen	2750	1050	1650	1005	1250	1700	1050	950	725	760
6.25 mm net	2560				1190				700	
Rollberg 6%,10%	2595,2807	1129,1153	2200,2335	1110,1190	1394,1556	1368,1584	1168,1323	1237,1454	767,825	1069,1153
Elas+B/30, 20%	2693,3230	1122,1261	2148,2448	1078,1258	1456,1704	1436,1797	1134,1470	1242,1630	754,874	1050,1226
Static										
Min/max skin	970,1244	412,614	803,1195	893, 1337	801,1055	559,970	444,621	647,847	469,682	482,731
Min/max point	216,1836	212,1435	280,2760	65,65	199,1377	211,1647	199,1176	200,1218	211,1435	228,1894
Min/max ultimate	1186,3080	624,2049	1083,3955	958,1402	1000,2432	770,2617	643,1797	847,2065	680,2118	710,2625
Dynamic										
Wave Eq. skin	1333/ 43%	500, 42%	1705, 55%	1075, 86%	636,53%	610,53%	506,46%	648,54%	696, 58%	600, 50%
point	1767/ 57%	700,58%	1395, 45%	175, 14%	564,47%	540,47%	594,54%	552,46%	504, 42%	600, 50%
ultimate	3100	1200	3100	1250	1200	1150	1100	1200	1200	1200

* Cohesive bearing layer

International Journal of Scientific & Engineering Research Volume 10, Issue 1, January-2019
ISSN 2229-5518

TABLE 7

Summary of the finite element method

Project No.	1	2	3	4*	5	6	7	8	9	10
Pile dimensions mm² x m	400²x24	285²x20	400²x23	285²x26	285²x26	285²x24	285²x21	285²x21	285²x21	285²x22
FEM										
Skin (kN)	1184	714	1118	1098	848	752	724	956	745	795
Point (kN)	1974	717	1202	135	602	618	716	579	690	655
Ultimate (kN)	3158	1431	2320	1233	1450	1370	1440	1535	1435	1450
Local sett. at ult. skin resist. (mm)	9 2.3% B	7.2 2.5% B	8 2% B	9.5 3.3% B	8.5 3.0% B	8 2.8% B	9.2 3.2% B	9.2 3.2% B	9.2 3.2% B	9.2 3.2% B
Butt sett. at ult point resist. (mm)	89 22.2% B	64 22.4% B	52 13% B	38 13.3% B	47 16.5% B	47 16.5% B	51 18% B	53 18.6% B	46 16% B	49 17% B
c_{u1} (kPa) / α_1	50/ 1.04	48/1.06	52/0.98	50/0.98	50/1.05	50/0.96	50/0.96	55/0.95	50/0.94	52/1.06
c_{u2} (kPa) / α_2	19/ 1.23	15/1.36	15/1.38	25/1.26	15/1.28	12/1.38	15/1.38	25/1.28	15/1.32	15/1.29
c_{u3}(kPa) / α_3	25/ 1.14			90/0.66		65/0.76				
N / φ^o	27/34	37/38	35/37		35/37	37/38	35/37	35/37	37/38	40/39
β	0.84	0.97	0.82		0.82	0.98	0.93	0.92	0.92	0.98
Unit skin (kPa)	194	186	181.3		98	217	182	189	170	124
Unit Point (kPa)	12339	8815	7512	1662	7411	7608	8511	7250	8221	8027

* Cohesive bearing layer

3. Davisson's, Brinch Hansen 90%, De-Beer's, Fuller-Hoy's, and Butler-Hoy's methods could not be applied for small settlement load test data ranges. The same is applicable for the (0.25 in) net-settlement criterion.

4. The ultimate pile capacities obtained from the load tests using Chin's method are almost equal to their counterparts obtained from Rollberg method at failure (plunging). Brinch-Hansen's (80%) and Van der Veen's methods give lower values.
5. The ultimate pile capacities obtained using the various static methods of predicting skin resistance and point bearing components, spread over a wide range.

6. Performing the analyses via the wave equation, as a dynamic method, produces good results. With a safety factor of (2.8), the allowable capacities of the driven piles are well estimated.
7. The results of GRLWEAP, revealed high stress levels induced in pile materials for some projects. It is recommended to consider (12 blows/in.) as a refusal condition.
8. The finite element analyses via PLAXIS show good agreement to the measured data. They produce failure loads, almost, similar to that obtained from Rollberg interpretation method.
9. The finite element analyses revealed local settlement of (2%B - 3.3%B) to mobilize the ultimate skin resistance. The computed unit skin friction ranges between (98 kPa) and (217 kPa).

10. The butt settlement values necessary to produce the ultimate frictional point resistance are (13%B - 22.4%B). The ultimate bearing stress range is (7250 kPa – 8815 kPa).

11. The suggested relations to predict the adhesion factors and skin friction parameters, as obtained from the finite element method, are shown in Figures (19 and 20).

12. Utilizing Figures (19 and 20) in calculating the ultimate skin resistance and Meyerhof's (1976) method in calculating the point bearing component, give appropriate allowable capacities, by applying a safety factor of (5). The maximum related settlement is (5.5 mm), which is equivalent to (0.6%B), and is accepted for most structures.

International Journal of Scientific & Engineering Research Volume 10, Issue 1, January-2019
ISSN 2229-5518

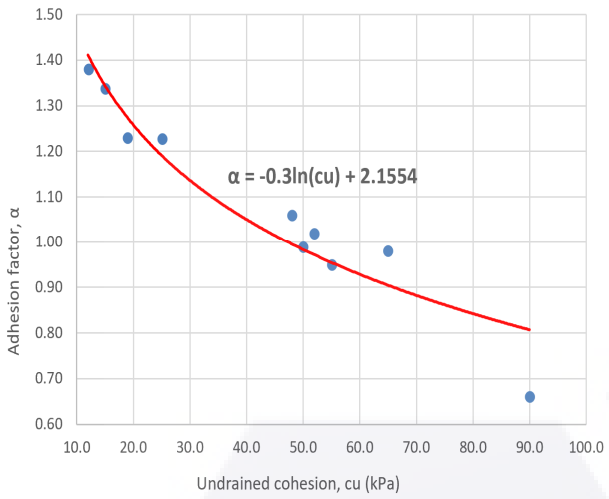

Fig. 19. Adhesion factors for driven piles in Basrah soil

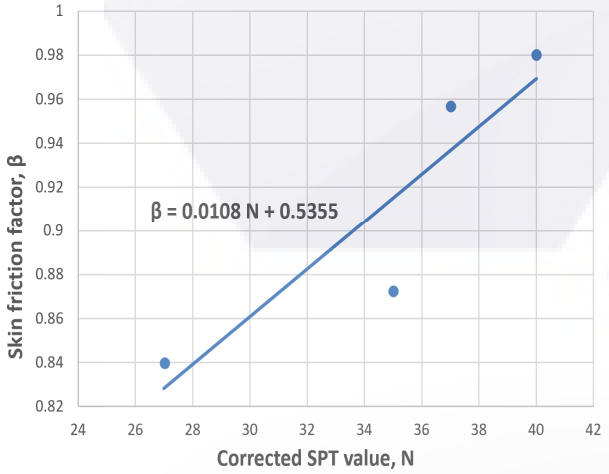

Fig. 20. Skin friction factor vs. standard penetration number for driven piles in Basrah soil

References

[1]. ASTM D1143/ D1143M, (2013), "Standard Test Methods for Deep Foundations Under Static Axial Compressive Load", 11 pp.

[2]. Bowles, J. (1997), "Foundation Analysis and Design-5th ed.", The McGraw-Hill Companies Corp, New York, St. Louise, 1168 pp.

[3]. Caltrans A. D. (2015), "Foundation Manual-2nd ed.", California Department of Transport, 522 pp.

[4]. Fleming, K. and Weltman, A. (2009), "Piling Engineering-3rd ed." ,Taylor and Francis Group, London and New York, 407 pp.

[5]. Gunaratne, Manjriker (2006), "The Foundation Engineering Handbook-st ed.", Tayler & Francis Group, Boca Raton, London and New York, 625 pp.

[6]. GRLWEAP (2010), "Theoretical Background Manual", 155 pp.

[7]. PLAXIS 3D Foundation (2015), "Scientific manual" , 66 pp.

[8]. Poulos H. and Davis E. (1980), "Pile Foundation Analysis and Design-1st ed.", Rainbow Bridge Co. Canada, 410 pp.

[9]. Prakash, S. and Sharma, H. (1990), "Pile Foundations in Engineering Practice-1st ed.", John Wiley & Sons, Inc. New York Chichester, 759 pp.

[10]. Rao, S.S. (2004),"Finite Element Method in Engineering-4th ed.", USA: Elsevier Science & Technology Books, 747 pp.

[11]. SHROF, A. AND SHAH D. (2003), "SOIL MECHANICS AND GEOTECHNICAL ENGINEERING-1ST ED.", A. A. BALKEMA PUPLISHERS. LISSE, ABINGDON, EXTON, TOKYO, 463 PP.

[12]. Tomlinson, M. and Woodward, J. (2015), "Pile Design and Construction Practice-6th ed.", Taylor and Francis Group, London and New York, 597 pp.

[13]. Viggiani, C. and Mandolini, M. (2012), "Piles and Pile Foundations-1st ed.", Spon Press, London and New York, 229 pp.

[14]. W.W. Li, and M. L. Cheng. (2006). "Foundation Design and Construction-1st ed.", The Government of the Hong Kong Special Administrative Region, first edition, 376 pp.

Site investigation and pile load test reports

[15]. University of Basra, Engineering Consulting Bureau, (March, 2008), "Soil Investigation Report, Kuwaiti Surgical Complex Hospital", (No. 1-SI-2008).

[16]. Al Fao Company for Geotechnical and Soil Investigation (March, 2013), "Pile Static Load Test Report, Kuwaiti Surgical Complex Hospital", (No. 511).

[17]. Andrea Engineering Test Laboratories (Nov, 2004), "Soil Investigation Report, Basra Children's Hospital", (No. 1051R).

[18]. Andrea Engineering Test Laboratories (Aug, 2005), "Pile Static Load Test, Basra Children's Hospital", (No. 511).

[19]. National Center for Construction Labs, (May, 2011), "Soil Investigation Report, Al-Mina'a Stadium", (No. 2-1-43).

International Journal of Scientific & Engineering Research Volume 10, Issue 1, January-2019
ISSN 2229-5518

[20]. Al-Tariq Engineering Bureau, (Feb, 2012), "Pile Static Load Test, Al-Mina'a Stadium", (No. 409).

[21]. University of Basra, Engineering Consulting Bureau, (May, 2013), "Soil Investigation Report,Shatt-Al Arab Central Water Treatment Plant", (No. 19/SI/2013).

[22]. Al-Meazan Co for Pile Test, (Aug, 2013), "Pile Static Load Test, Shatt-Al Arab Central Water Treatment Plant", (No. 95).

[23]. University of Basra, Engineering Consulting Bureau, (May, 2008), "Soil Investigation Report,Al Basra West Electrical Substation (132 kV)", (No.6/SI/2008).

[24]. National Engineering Contracts, (Jan, 2010), "Pile Static Load Test, Al Basra West Electrical Substation (132 kV)", (No. Jan-2010).

[25]. National Center for Construction Labs, (Aug, 2013), "Soil Investigation Report,Shatt Al Arab Hospital", (No. 2-1-44).

[26]. Al-Liqa'a Engineering Bureau, (Jan, 2013), "Pile Static Load Test, Shatt Al Arab Hospital", (No. 364).

[27]. National Center for Construction Labs, (June, 2011), "Soil Investigation Report,Health Care Center", (No. 2-1-43).